Investigations of property-controlled flow forming with defined strain hardening using a virtual sensor

Jeannette BOLL[1,a *], Robert LAUE[1,b], Frank WENDLER[2,c], Carolin BINOTSCH[1,d], Till CLAUSMEYER[1,e], Sebastian HÄRTEL[3,f], Olfa KANOUN[2,g] and Birgit AWISZUS[1,h]

[1]Professorship Forming Technology, Chemnitz University of Technology, Reichenhainer Str. 70, 09126 Chemnitz, Germany

[2]Professorship Measurement and Sensor Technology, Chemnitz University of Technology, Reichenhainer Str. 70, 09126 Chemnitz, Germany

[3]Chair of Hybrid Manufacturing, Brandenburg University of Technology, Konrad-Wachsmann-Allee 17, 03046 Cottbus, Germany

[a]jeannette.boll@mb.tu-chemnitz.de, [b]robert.laue@mb.tu-chemnitz.de, [c]frank.wendler@etit.tu-chemnitz.de, [d]carolin.binotsch@mb.tu-chemnitz.de, [e]till.clausmeyer@mb.tu-chemnitz.de, [f]sebastian.haertel@b-tu.de, [g]olfa.kanoun@etit.tu-chemnitz.de, [h]birgit.awiszus@mb.tu-chemnitz.de

Keywords: Flow-Forming, Property-Controlled, Finite Element Method (FEM), Incremental Forming, Strain Hardening, Subroutine

Abstract. The advantage of (incremental) cold forming processes is that, in addition to the component geometry, the mechanical and physical properties can also be positively influenced. Appropriate control during the forming process is necessary to produce components with a defined geometry and defined, optimized product properties. To produce components with defined (graded) strain hardening by flow-forming a sensor for measuring the strain hardening was developed. Based on the measurement of magnetic permeability and magnetic anisotropy, control instructions are derived and forwarded to an actuator. Numerical simulation with Simufact Forming is used to evaluate the overall system and analyze the optimization of the product properties. In addition to the simulation of the flow-forming process, a virtual sensor for the strain hardening is applied based on the measurement of the experimental investigations. A subroutine was used to automatically adjust the roller feed within the simulation so that components with predefined hardening could be produced. The FE model is further used to optimize the real sensor position and functionality.

Introduction

In the context of sustainability and resource efficiency, product tolerances and production standards are becoming increasingly stringent. As a result, monitoring and controlling metal forming processes is gaining importance. While forming processes already utilize closed-loop controls for inline process adjustments, there is still a need to implement such controls for managing the product properties of the components [1, 2, 3]. By integrating closed-loop controls that provide feedback on microstructure evolution (and thus product properties), forming processes can be designed to be more efficient and sustainable [4].

The advantage of (incremental) cold forming processes is that, in addition to the component geometry, the mechanical and physical properties can also be positively influenced. Appropriate control during the forming process is essential to produce components with a defined geometry and defined, optimized product properties. The control of forming machines is usually limited to controlling the movement sequences. The processes are mainly controlled in terms of their effect on the product properties, but cannot interact with this effect. This means that it is not possible to readjust the process parameters due to fluctuations in the workpiece properties or interferences caused by the process boundary conditions during forming [5].

The goal of this study is to control forming processes based on their product properties, enabling a response to changing boundary conditions, disturbances within the forming process and fluctuations in the starting material. Therefore, the forming process is independent of external disturbance variables and components with the same geometry but different product properties (strain hardening) can be produced. This type of control is particularly relevant for low-volume processes (e.g., incremental processes), as in-process measurement and control help to reduce defects. Additionally, property-controlled forming allows for the automatic generation of forming kinematics in real-time, based on the product properties, without the need for prior calculations.

This paper presents an investigation of property-controlled flow forming using the finite element method (FEM). It explains the experimental and numerical measurement processes for strain hardening, as well as the integration of a virtual sensor through the use of a subroutine.

Incremental Flow Forming

In the incremental flow-forming process, the mandrel is attached to the main spindle of the machine and is set in rotation together with the semi-finished product. A freely mounted roller also rotates on contact with the workpiece due to friction. As the radially adjusted roller continuously moves forward (axial feed), the outer diameter of the semi-finished product decreases, resulting in axial elongation of the component in opposite feed direction (Fig. 1).

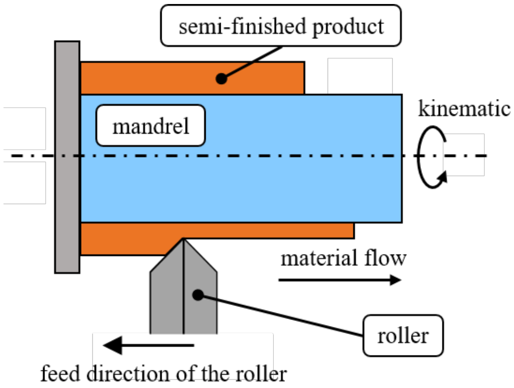

Figure 1 – Schematic of flow-forming with opposite material flow

Property-Controlled Flow Forming

The focus of property-controlled flow-forming is to control the forming process based on the product property of strain hardening. In the incremental flow-forming process, the reduction in wall thickness and axial extension within the tube wall results in strain hardening due to the forming process. Based on the measured strain hardening, the roller feed (axial feed per workpiece rotation) is controlled to achieve the desired strain hardening in the component. Altering the roller feed rate affects the material flow and therefore the strain hardening without changing the component geometry. In general, a low roller feed rate results in a high plastic strain and high roller feed rate in a lower plastic strain [4].

In previous studies, a new multi-modal sensor system, consisting of a hardware sensor, a softsensor and a controller, had to be developed as no sensor existed that could measure strain hardening [4, 6, 7, 8]. The sensor consists of commercially available coils with an outer diameter of 9 mm for the sensing coil and 2 mm for the receiver coils for determining the relative magnetic permeability and magnetic anisotropy and an additional temperature sensor [7]. The concept of coevolution of mechanical and magnetic properties of ferromagnetic materials under plastic strain was applied to the sensor system. As the plastic strain increases, the associated defects in the material increase. As a result, mechanical embrittlement coincides with magnetic embrittlement. This reduces the adaptability to external magnetic fields, which corresponds to the magnetic permeability. Furthermore, the directional magnetizability changes according to the direction of the applied mechanical stress due to the Villari effect (magnetic anisotropy) [9, 10]. Both magnetic properties can be measured in a single measurement. Due to the sensor size and roller positioning, it is not possible to measure directly in the forming zone below the roller. Furthermore, the axial measuring position behind the forming zone was necessary so that the measuring surface can be geometrically described by the sensor. Therefore, an indirect measurement is used, which results in a time offset between the development of the property and the property measurement [11].

The single measurement of the magnetic properties of the tube is carried out without contact during the forming process by the hardware sensor (Fig. 2). For a robust measurement, the sensor detects changes in the distance to the component and provides data on the tilting of the sensor during the measurement. Then the softsensor, equipped with an internal material model, utilizes information on magnetic anisotropy and changes in magnetic permeability to estimate the plastic strain. Since the correlation between the magnetic properties and the strain hardening is described in the softsensor, as is the correlation between the relative feed rate and the strain hardening, the measurement of the magnetic properties can be used to draw conclusions about the strain hardening achieved by adjusting the feed rate. Finally, the softsensor sends a feedback for the control loop of the forming process and regulates the roller feed rate depending on the desired strain hardening.

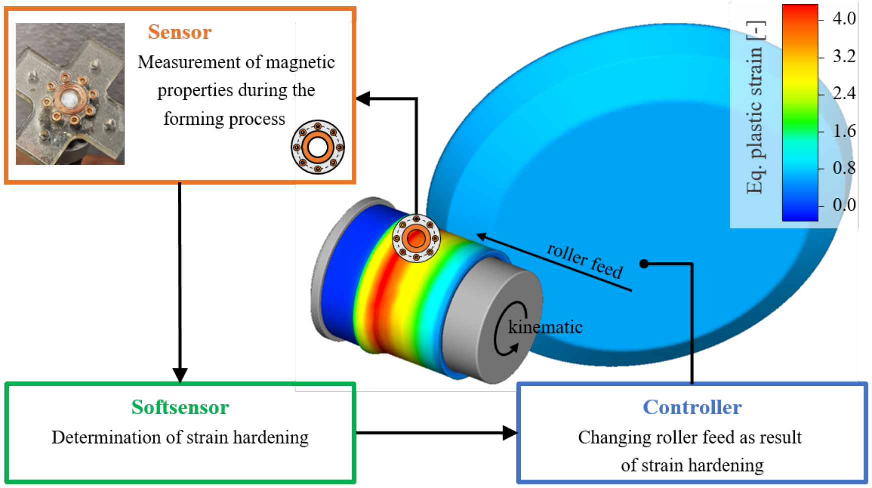

Figure 2 – Schematic process flow of the property control

The realization of the closed-loop control measuring strain hardening during flow-forming is shown schematically in Fig. 3. The control is achieved by using an additional external control loop (strain hardening control) alongside the existing internal control loop of the forming machine (tool kinematics). The external control loop carries out the measurement of the magnetic properties, which are then processed by a microcontroller. The softsensor performs the strain hardening calculation. The result is then compared to the predefined target product property. If a deviation is detected, the calculated control data (instructions for adjusting rotational speed and feed) are then implemented by the machine's internal control loop. The actuator changes the roller feed and rotational speed to achieve the desired strain hardening. This is followed by a new measurement of the current product property.

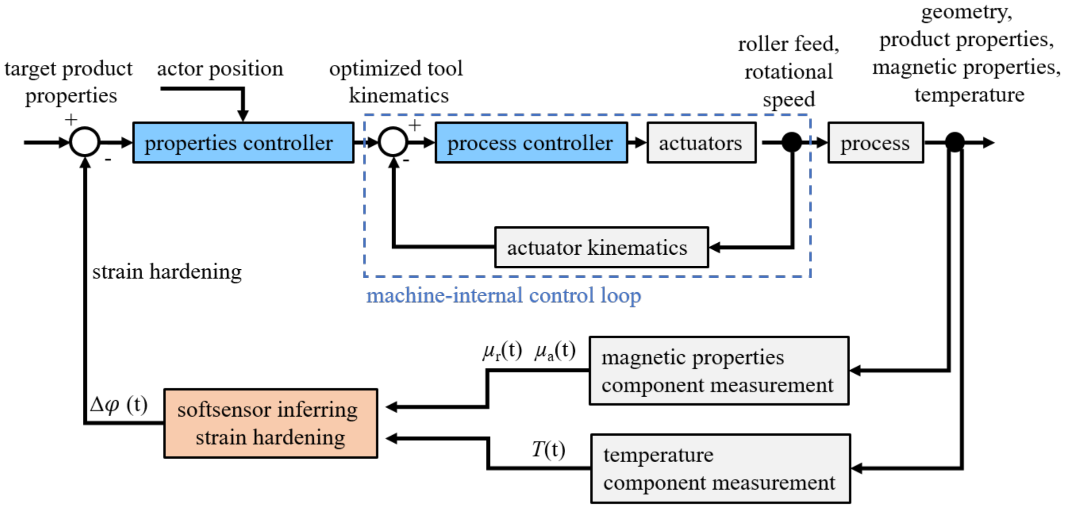

Figure 3 – Closed-loop control measuring concept during flow-forming

Numerical simulation

A numerical model (Fig. 4) in the Simufact Forming software (Hexagon, Stockholm) using an implicit equation solver was developed, in order to analyze the regulation of the hardening in more detail.

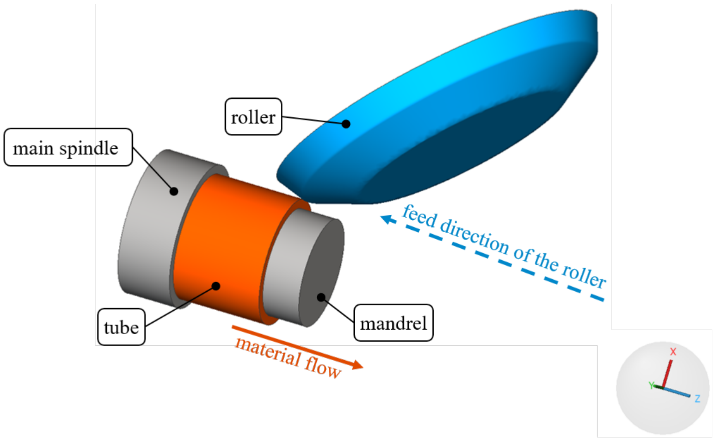

Figure 4 – FE model developed in the Simufact Forming software

A three-dimensional FEM model is used to represent the incremental forming process due to the kinematics of the process. Mandrel, roller and main spindle are defined as rigid bodies without thermal conduction. The main spindle is used as a simplification and replicates the clamping of the tube. Mandrel and main spindle are set in rotation with a rotational speed of 300 rpm. The kinematic of the roller corresponds to the CNC control data of reference components, which is implemented in the simulation model through a table. The roller feed rate is 30 to 150 mm/min (0.1 – 0.5 rpm).

The start geometry of the component includes a length of 50 mm, an outer diameter of 70 mm, and a wall thickness of 5 mm. The mandrel diameter is 59.99 mm. The material used for the work piece is E235+N. The material properties were characterized using compression tests [12]. Based on the experimentally determined flow curves for the process-relevant range, an analytical flow curve approach according to Hensel-Spittel (Eq. 1) was used, with the following coefficients: A = 628.904, m_1 = -0.0008176, m_2 = 0.0765987, m_3 = 0.0021320, m_4 = -0.0069053, where φ represent the equivalent plastic strain and T the temperature, respectively.

$$k_F = A * e^{m_1 * T} * \varphi^{m_2} * \dot{\varphi}^{m_3} * e^{\frac{m_4}{\varphi}}. \tag{1}$$

Regarding the discretization of the workpiece it is necessary to use volume elements (8-node hexahedron) for the tube, due to the three-dimensional stress state in the forming zone. These are arranged as a regular ring mesh with a homogeneous distribution and a mesh size of 1.25 mm.

For rotational processes, the time step should be selected so that the rotation angle per time or calculation increment does not exceed an angle of 5°. In the FE model, the rotation angle of the workpiece was selected to correspond to the angle of the element (2.5°). This is important when considering contact, where a node-segment contact is used. It checks the penetration of each node of the tools into segments of the workpiece. The chosen angle ensures that one node of the workpiece is always located under the roller [12]

Other boundary conditions are friction and heat transfer. A combined friction model consisting of Coulomb and Tresca friction laws is used. The coefficients are based on previous studies by Kleditzsch [13]. The friction coefficients are set to $\mu = 0.08$ for Coulomb and $m = 0.15$ for Tresca. The heat transfer coefficients were determined through experiments where either the tool or the workpiece was heated, and then the cooling process was measured. This investigation was also simulated using numerical methods, and the heat transfer coefficient was adjusted until the temperature curves showed deviation of less than 5 % [12]. The thermal radiation with a material constant of 0.9 and the thermal conduction within the tube were taken from the database. To reduce the calculation time, the mandrel and roller were implemented without thermal conduction, meaning with a constant temperature during the forming process.

Extension of the FE model with a virtual sensor

For a better investigation of the control process, a virtual sensor was added to the evaluated FE model. This sensor evaluates the equivalent plastic strain at the measurement position of the real sensor during the simulation. Subsequently, the instruction for adjusting the rotational speed is calculated in a virtual controller. A new developed subroutine written in Fortran was used to make the necessary user-defined adjustments in the solving process. It can be executed at various points during the iterative simulation. Through a subroutine it was possible to implement a method in the numerical simulation that reproduces the behavior of the real sensor. Similarly, based on the equivalent plastic strain obtained for local points in the subroutine, analogously to a real actuator, process parameters can be adjusted in the simulation. A special feature of this procedure is that measurement and control take place during the solving process of the simulation.

A separate subroutine is used for both the external control loop (virtual sensor) and the internal machine control loop (Fig. 5, a). The exchange of control commands between the subroutines occurs through the temporary storage of data in an external memory. The subroutine for the virtual sensor (Fig. 5, b) is executed before each increment, so it is not included in the iteration cycle.

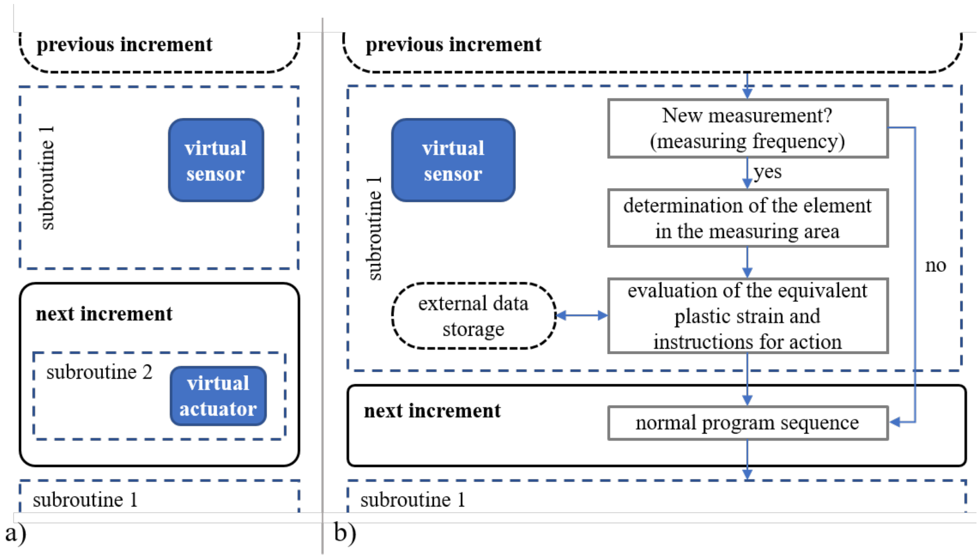

Figure 5 – General schematic sequence of the subroutines: a) overview of the control measuring concept, b) detailed view of the virtual sensor

Before a measurement of the equivalent plastic strain is carried out by the virtual sensor, it is first checked whether the measurement time (based on the measuring frequency) has been reached. The measurement frequency of the virtual sensor corresponds to the measuring frequency of the real sensor system. It is determined by the time required to measure the magnetic properties and calculate the control, or it corresponds to the actuator's response time. In reality the roller feed rate can only be changed again after the actuator has performed the previous adjustment. With this scheme the simulation-based virtual sensor and actuator are synchronized with the softsensor in the real experiments. It ensures that the minimum response time of the real measurement and control system is not exceeded [12]. If the measurement time has not yet been reached, the program proceeds with the normal program sequence. However, if the measurement time is correct, all nodes of the workpiece are considered sequentially. In a do-loop, it is first checked whether the node is located in the outer area of the workpiece. Since the real sensor only measures near the surface, only these nodes in the simulation are taken into account for the equivalent plastic strain measurement. If the considered node is close to the surface, the exact position of the node is then determined to check, whether it lies within the sensor's measurement range. The measurement range is defined as being next to the flow forming roller and covers an area within a diameter of 13 mm (see Fig. 2). If the node is within the measurement range, the equivalent plastic strain of the corresponding element is evaluated.

Correlation between measuring point and final equivalent plastic strain

Since the real sensor cannot be positioned directly beneath the roller in the forming zone, there is a time offset between the development of the property and its measurement. This temporal and spatial offset is presented in Fig. 6. It shows the development of the tube radius in comparison to the evolution of the equivalent plastic strain during the forming process. The peak of the radius represents the pile-up geometry beneath the roller in the forming zone ($t = 2 - 3$ s), where the final equivalent plastic strain is influenced und also changes in the roller feed rate have impact on. At approximately 5.5 seconds the final radius as well as the final equivalent plastic stain is reached. The forming process is completed at this point and it is no longer possible to influence the final equivalent plastic stain as part of the control process.

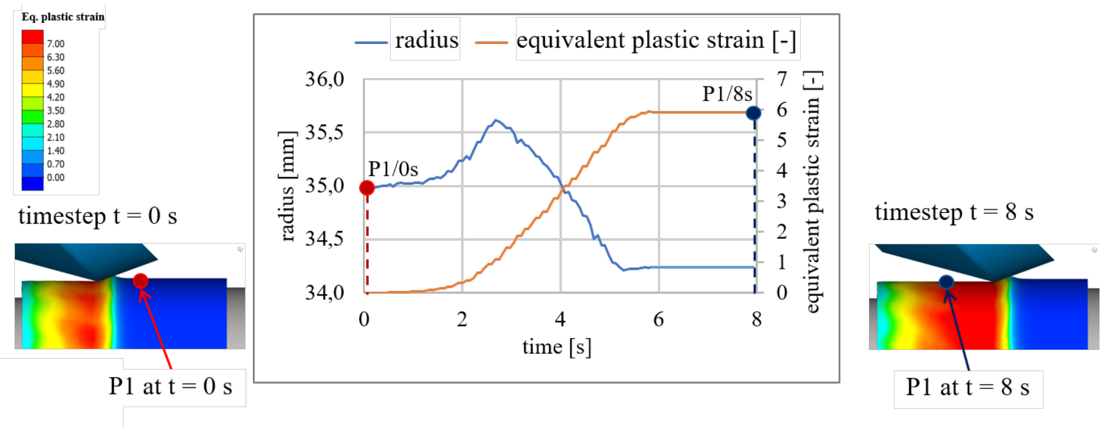

Figure 6 – Correlation between the evolution of geometry and equivalent plastic strain in FE model

Therefore, the FE simulation is used to analyze the correlation between the measured equivalent plastic strain at time t_1 and t_{End}. The approach used in the study is shown in Fig. 7.

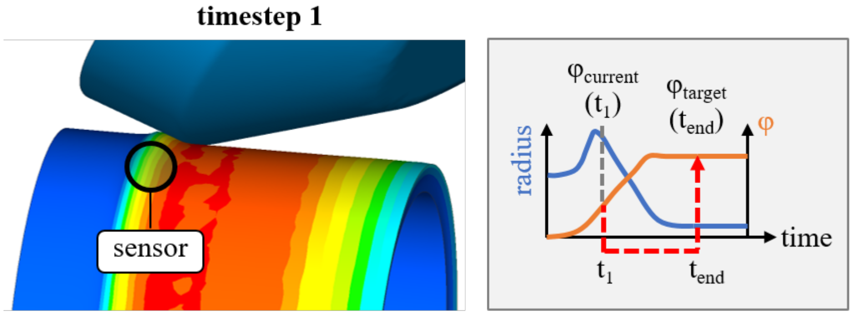

Figure 7 – Determination of the correlation between the measured equivalent plastic strain (φ) at time t_1 and t_{End}

The aim is to find out, if the equivalent plastic strain assumes a certain value at time t_1, what value results from this for the equivalent plastic strain at time t_{end}. This allows the softsensor and the control system to be set more precisely in the real process. An important aspect that must be evaluated is the elongation of the workpiece during forming due to the reduction in wall thickness. Consequently, a measurement at position x results in position $(x+y)$. It is also necessary to know the extent to which the equivalent strain reacts to changes in the roller feed rate. The combination of the various correlations can only be analyzed by means of simulation.

Discussion of results

The investigations using the virtual sensor were carried out based on an evaluated reference simulation with different feed rates of 0.1, 0.3, and 0.5 rpm (30, 90 and 150 mm/min). Fig. 8 (a) shows the equivalent plastic strain of the feed rate 0.3. It shows that the equivalent plastic strain is homogeneously distributed around the circumference for a given axial position. Thus, the desired axial variation of different, annularly arranged forming zones can be achieved (Fig. 8, b). Furthermore, the equivalent plastic strain can be measured at t_{end} in axial direction without problems. Geometrically, the pile-up geometry beneath the is recognizable, which is followed by the quasi-stationary state in the axial direction.

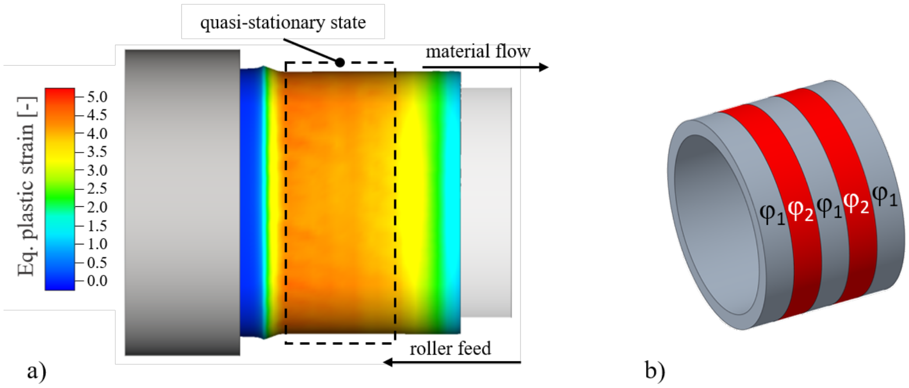

Figure 8 – a) equivalent plastic strain at a roller feed rate of 0.3 rpm in FE simulation, b) axial variation of annularly arranged equivalent plastic strain

The equivalent plastic strain was measured with the virtual sensor to establish whether there is a correlation between the measured values (t_1) and the values at t_{end}. In addition, the equivalent plastic strain was measured axially over the final component (equivalent plastic strain at t_{end}). The diagrams in Fig. 9 show the equivalent plastic strain over the workpiece length on the one hand at the location of the virtual sensor (t_1) and on the other hand at the time of the final forming step (t_{end}).

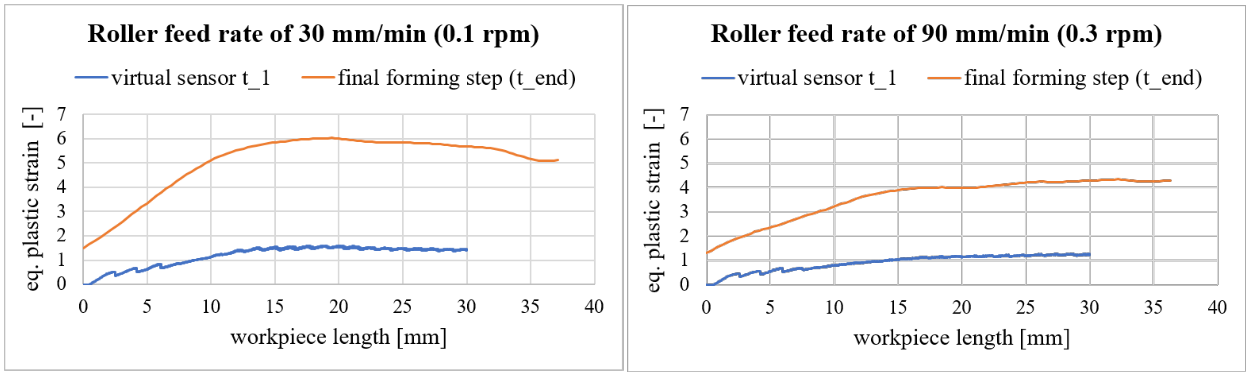

Figure 9 – Equivalent plastic strain during measurement (virtual sensor t_1) and at the end (final forming step t_{end})

The diagram on the left shows the simulation at a roller feed rate of 30 mm/min (0.1 rpm) and the diagram on the right at a feed rate of 90 mm/min (0.3 rpm). Both diagrams show that the curves for t_1 and t_{end} are similar. This suggests that there is a correlation between the values. The equivalent plastic strain values of the virtual sensor start at zero. The equivalent plastic strain then gradually increases during the formation of the pile-up geometry under the roller (up to about 15mm), after which a quasi-stationary state develops, where no further or only slight changes in the forming degree occur. In the quasi-stationary state, the virtual sensor measures a forming degree of 1.2 for a roller feed rate of 0.3 rpm. The final equivalent plastic strain at t_{end} in the quasi-stationary region is 4. This can be explained by the fact that at the time of the virtual sensor measurement, the final wall thickness has not yet been reached, and the plastic deformation is not yet complete.

The offset of the curves along the workpiece length results from the elongation of the workpiece during forming. This clearly shows that the elongation of the workpiece during forming due to the reduction in wall thickness must be considered when analyzing the correlation between t_1 and t_{end}. To address this, the amount of elongation in axial direction must first be calculated. This can then be transferred to the target design.

Summary

This work presents the property-controlled flow forming and its implementation as an FE model in Simufact Forming. It showed the experimental control loop of measuring strain hardening during flow forming using a multi-modal sensor system. Furthermore, a newly developed method, which was implemented with a subroutine, has been presented that simulates the measurement task of a physical sensor within an FE model.

With the implementation of the virtual sensor, it could be shown that there is generally a correlation between the equivalent plastic strain at the position of the virtual sensor and the final equivalent plastic strain. Therefore, an indirect measurement of the component properties can be used. However, it was also shown that the component elongation during flow forming in opposite feed direction must be considered when examining the correlation. In further numerical studies additional feed rates and reduction ratios (thickness reductions) need to be conducted. After that the new control method must be integrated in the softsensor and finally evaluated in experimental studies. This is intended to lead to the development of a control instruction for property-controlled manufacturing of components with defined strain hardening by flow forming in subsequent studies. This allows producing components with different strain hardening (material properties) but the same geometry, regardless of the boundary conditions.

Acknowledgement

The authors would like to thank the German Research Foundation for funding the project “Controlled flow forming for production of workpieces with a defined strain hardening” (project number 424334154) as part of the SPP2183: Property-controlled metal forming processes.

References

[1] W. Hao, S. Duncan, Optimization of tool trajectory for Incremental Sheet Forming using closed loop control, 2011 IEEE International Conference on Automation Science and Engineering, Trieste, Italy, 2011, pp. 779-784. https://doi.org/10.1109/CASE.2011.6042410

[2] M. Bambach, T. Meurer, W. Homberg, S. Duncan, Editorial to special issue “Property-controlled forming processes.”, Advances in Industrial and Manufacturing Engineering. 4 (2022). https://doi.org/10.1016/j.aime.2022.100068

[3] J.M. Allwood, S.R. Duncan, J. Cao, P. Groche, G. Hirt, B. Kinsey, T. Kuboki, M. Liewald, A. Sterzing, A.E. Tekkaya, Closed-loop control of product properties in metal forming, CIRP Annals. 65 (2016) 2, pp. 573-596. https://doi.org/10.1016/j.cirp.2016.06.002

[4] S. C. Stebner, J. Martschin, B. Arian, S. Dietrich, M. Feistle, S. Hütter, R. Lafarge, R. Laue, X. Li, C. Schulte, D. Spies, F. Thein, F. Wendler, M. Wrobel, J. R. Vasquez, M. Dölz, S. Münstermann, Monitoring the evolution of dimensional accuracy and product properties in property-controlled forming processes, Advances in Industrial and Manufacturing Engineering. 8 (2024). https://doi.org/10.1016/j.aime.2023.100133

[5] J. M. Allwood, J. A. Polyblank, S. R. Duncan, Closed-loop control of product properties in metal forming: A review and prospectus, Journal of Materials Processing Technology. 214 (2014) 2333-2348. https://doi.org/10.1016/j.jmatprotec.2014.04.014

[6] F. Wendler, R. Laue, S. Härtel, O. Kanoun, B. Awiszus, Multifrequency Multichannel Eddy Current Sensor System for the Analysis of Mechanical States in Ferromagnetic Materials, Proceedings Sensor and Measurement Science International 2023 Conference. (2023) 203-204. https://doi.org/10.5162/SMSI2023/D1.4

[7] F. Wendler, R. Laue, S. Härtel, B. Awiszus, O. Kanoun, Design of a multi-modal sensor for the in-process measurement of material properties based on inductive spectroscopy, Measurement. 227 (2024). https://doi.org/10.1016/j.measurement.2024.114187

[8] W. Homberg, B. Arian, V. Arne, Softsensors: key component of property control in forming technology, Production Engineering Research Development. 18 (2024) 603-614. https://doi.org/10.1007/s11740-023-01227-1

[9] C. Joh, J. W. Lee, I. Kwahk, Feasibility Study of Stress Measurement in Prestressing Tendons Using Villari Effect and Induced Magnetic Field, International Journal of Distributed Sensor Networks. 9 (2013) 11. https://doi.org/10.1155/2013/249829

[10] R. Laue, F. Wendler, S. Härtel, O. Kanoun, B. Awiszus, Analysis of stress influence and plastic strain on magnetic properties during the forming process. Advances in Industrial and Manufacturing Engineering. 3 (2021). https://doi.org/10.1016/j.aime.2021.100053

[11] R. Laue, F. Wendler, S. Härtel, B. Awiszus, O. Kanoun, Eigenschaftsgeregeltes Drückwalzen im digitalen Zwilling, Proceedings Ideen Form geben - 36. ASK Umformtechnik. (2022) 349-358.

[12] R. Laue, Entwicklung des selbstregelnden Drückwalzens, Dissertation, TU Chemnitz, Berichte aus der Virtuellen Fertigungstechnik, 19 (2024)

[13] S. Kleditzsch, Beitrag zur Modellierung und Simulation von Zylinderdrückwalzprozessen mit elementaren Methoden. Dissertation, TU Chemnitz, Berichte aus der Virtuellen Fertigungstechnik, 11 (2014)